An Advanced Control Strategy for the Evaporation Section of An Integrated First- and Second-Generation Ethanol Sugarcane Biorefinery

E. Y. Emori, M. A. S. S. Ravagnani, and C. B. B. Costa*
Chemical Engineering Department,
Universidade Estadual de Maringá,
Av. Colombo, 5790 Bloco D90, CEP 87020-290,
Maringá, PR, Brazil

doi: https://doi.org/10.15255/CABEQ.2022.2048

Original scientific paper
Received: January 5, 2022
Accepted: January 26, 2023

The sugarcane crushing stage is one of the most important technologies being developed at the moment. In this paper, the control of the multiple-stage evaporation system was addressed, as it is a crucial stage in the first- and second-generation ethanol production from sugarcane. A neural network model was proposed based on a dynamic phenomenological model developed in EMSO (Environment for Modeling, Simulation and Optimization). The phenomenological model was used to build a neural network prediction model for an MPC (Model Predictive Control) scheme using a DMC (Dynamic Matrix Control) algorithm. Simulations were carried out to evaluate the performance for tracking the set-point. Also, disturbance rejection tests were performed, considering different step disturbances. The analysis demonstrated that the MPC scheme performed well in the tests and showed superiority when compared to classical PID controllers.

Keywords
model predictive control, neural network, multiple-stage evaporation, EMSO, second-generation ethanol, dynamic matrix control

Introduction

Sugarcane processing is one of Brazil's most significant economic operations. It has enabled the country to become the world's second-largest manufacturer of bioethanol, accounting for about 27 % of global output. Ethanol production from sugarcane in Brazil is one of the most competitive sectors of the national and world economy, with 422 sugarcane factories operating all around the country[1,2]. Within the 2020/2021 harvest season, over 657.4 Mt of cane were used as feedstock, producing more than 41.5 Mt of sugar and 32.5 Mm^3 of ethanol[3]. A large byproduct of alcohol production is bagasse, which is burned to produce steam in boilers. This steam is then used as a utility in different sectors of the plant. Second-generation ethanol production from bagasse has an inexpensive raw material and is an environmentally friendly alternative to rising ethanol production[4]. However, in comparison to first-generation substrates[1], lignocellulosic materials are more difficult to be processed because of their heterogeneous composition and sophisticated structure. Since the three components of lignocellulose (cellulose, hemicellulose, and lignin) are so closely linked, pretreatment and enzymatic hydrolysis are required prior to fermentation to enable the sugars contained in the cellulose and hemicellulose compounds to be released[4,5].

The production process of bioethanol consists of two main parts in general: the first- and second-generation processes. In the first-generation process, sugarcane juice is extracted in mills, pre-treated, clarified, concentrated in evaporators, and then fermented and distilled. In second-generation ethanol production, sugarcane bagasse is used as feedstock. This biomass passes through pre-treatment and hydrolysis processes that transform the cellulose fraction of biomass into a hexose syrup. This syrup is then fermented and distilled to obtain ethanol[6]. From both production processes, evaporation is one of the most energy-consuming stages. Due to the high latent heat, evaporation of water consumes a huge amount of thermal energy and fuel, which results in high operating costs and environmental problems[7].

For the development of biofuels, lignocellulosic biomass provides the most accessible, carbon-neutral alternative resource. It is the most appropriate carbon-based feedstock due to its abundance and renewable nature. Also, the production of lignocellulosic products is possible without increasing the cultivation area, therefore there is no

*Corresponding author: Caliane Bastos Borba Costa, ORCID: 0000-0002-9983-566X E-mail: cbbcosta@uem.br

overlap with the food industry. Processing lignocellulosic biomass is environmentally friendly since it ensures that most components are processed into valuable products[8]. Bioethanol made from lignocellulose is regarded as a viable alternative to fossil fuels, and its market is expected to grow as a result of its widespread use as a fuel additive. Another advantage of using bagasse as feedstock for bioethanol production in sugarcane industries is its ready availability at the plant site. Also, second-generation bioethanol production may share part of the infrastructure where first-generation ethanol production takes place (for instance, concentration, fermentation, distillation, storage, and cogeneration facilities)[4,5]. In addition, potential fermentation inhibitors generated during the pretreatment of the lignocellulosic material might have a weakened impact on fermentation yields, since a dilution of those inhibitors occurs when the hydrolyzed liquor is mixed with sugarcane juice and fermented simultaneously[6].

In dairy, sugar, medicine, and a variety of other sectors, the multiple-stage evaporator (MSE) is commonly used. Controlling an MSE effectively results in higher product quality and lower energy costs. The purpose of the evaporation process is to ensure that the product brix quality is maintained. Unwanted characteristics, such as time delays, powerful disturbances, and coupling effects, on the other hand, add uncertainty and make control challenging[9]. Despite the complexity and non-linear dynamic of the process, it is quite common to find only PID control on industrial applications of such a piece of equipment. Classical PID usage is explained by its well-structured theory, simple implementation and tuning, and high versatility to deal with wide types of process variables. Despite its high versatility, PID control alone may have some inefficient aspects, such as unsuitability for nonlinear behavior and a lack of predictive actions to disturbance effects in regulatory control once its control algorithm is based only on the controlled variable error[10].

Many authors have reported different control strategies applied to sugarcane juice multiple-stage evaporators, using simulation as a testing tool. As it is a very versatile problem, diverse approaches are found in the literature. Adams *et al.*[11] enhanced the poor control structure commonly used in the sugarcane industry by developing a feedforward scheme. That paper focused on problems presented by a double-stage evaporator caused by brix and level disturbances. Pérez *et al.*[12] studied a five-stage evaporator of a sugarcane operating plant and proposed a mathematical model of that system and its control scheme with PID controllers, but a high stabilization time was observed due to the high dead time of the evaporator stages. Ahammad *et al.*[13] reported different applications of fuzzy controllers in multiple-stage evaporators of a sugarcane plant. Merino *et al.*[14] implemented Real-Time Optimization (RTO) in a sugar cane industry evaporator. In order to find optimal operating conditions, the algorithm uses data validation, reconciliation, and optimization.

From the many different schemes found in the literature, Model Predictive Control (MPC) stands out in the control of multiple-stage evaporation systems. Because of its capacity to manage restrictions, range control, and plants with complicated behavior, MPC technology is presented as a typical solution for industrial multivariable systems, mainly when constraint fulfillment and control performance optimization are required. Its implementation is based on a representative process model-based solution to an open-loop finite-horizon control issue. From this model, the controller estimates a sequence of control actions for each sample instant, guiding the process toward its optimal path. MPC has the advantage of being able to improve operational performance by reducing system unpredictability. It has the ability to maximize high-value product recovery, enhance plant capacity while operating under restrictions, and reduce energy usage[15,16]. Smith *et al.*[17] modeled a five-stage evaporator of a sugarcane factory, and the model was used as an internal model for a model predictive controller[17]. Benne *et al.*[18] applied advanced control in a five-stage evaporator. The method used an MPC scheme with a black-box neural network as a prediction model. Ipanaque *et al.*[19] studied the modeling, simulation, and nonlinear control of a double-stage evaporator of a sugarcane bioethanol plant. Nonlinear Generalized Predictive Control (GPC) was used to control the juice concentration at the output of the last evaporator stage. Acebes *et al.*[20] focused on plant-wide control with a three-stage evaporator as its key central system using a dynamic nonlinear MPC supported by PID controllers, along with an algorithm that calculated the dynamic scheduling of the production process. Mazaeda *et al.*[21] also applied MPC in plant-wide control of a sugar factory, working with the last three stages of the evaporation system.

As noted, there are many different applications of MPC in the control of multiple-stage evaporation systems. Although many of them are concerned with the sugarcane industry, there is no study related to integrated first- and second-generation ethanol production. This integration changes the process and adds distinct features that can be an obstacle to the proper operation and the success of the control system. The addition of a glucose syrup flow rate changes the juice composition and is a source of disturbance, due to variations in units that promote

the processing of the lignocellulosic material (pre-treatment, enzymatic hydrolysis, filtering, etc.). Also, syrup flow interruptions may be necessary due to operational issues. Furthermore, the effective control of evaporators in the integrated biorefinery becomes very important because a significant part of what was previously available fuel for steam generation (bagasse) is being used as raw material for second-generation ethanol, so that the use of steam cannot be indiscriminate. Therefore, the control scheme and configuration for such a process is an interesting subject of study.

When using MPC, the model that is utilized for the prediction can be obtained in a variety of methods. While some prefer to specify the model in advance, it is frequently more feasible to do system identification and fit a model based on observed input-output behavior. Nonlinear MPC techniques often use black-box models to predict the system behavior due to its cheaper computational cost[22]. The usage of black-box models for MPC is advantageous nowadays with the progress of computational processing. Since they do not require a knowledge of system physics, black-box models are relatively simple to set up. In order to train these models, a comprehensive collection of system input-output data under reasonable working conditions is necessary. As a result, the ease with which inverse models can be developed comes at the expense of reduced generalization capability when compared to phenomenological models. Of all nonlinear black-box modeling techniques available, Artificial Neural Network (ANN) is the most common modeling method due to its high reliability in modeling nonlinear systems as compared to other methods. ANN uses multiple layers of neurons to replicate the human brain. In most cases, supervised learning techniques are used to train the weights of these neurons. An ANN that has been properly trained can accurately approximate any nonlinear operation[23]. One of the most common neural networks is the backpropagation neural network (BPNN). It has three layers and is a standard multilayer perceptron (MLP). It has been widely used in numerous fields due to its high nonlinear processing capability[23,24]. In this context, a black-box model is suitable to represent a multiple-stage evaporator model due to its nonlinear dynamics. One of the most successful MPC methods and widely used in the industry is the Dynamic Matrix Control (DMC) algorithm. This method uses a model step response, which is set for a particular operating point in the system. The control signals are defined by the minimization of an objective function that contains the predicted data, and the model of the process is used to predict future outputs throughout a prediction horizon. In practice, the DMC algorithm provides better control quality (e.g., smaller overshoots or a lower settling time) than traditional PI or PID controllers, particularly for plants with large time delays[25].

Most works presented previously used commercial simulators. Contrary to the previous pieces of software employed in the works mentioned here, EMSO is a piece of software with an uncharged license for academic research and educational activities. Also, it has the advantage that all built software models are available for inspection and extension by any user, making it extremely versatile for scientific use. It has a graphical interface for modeling techniques based on block diagrams, as well as a modeling language with object-oriented features, which enables the hierarchical inclusion of parameters, variables, and equations to enhance model complexity. It also has a broad range of applications, including steady and dynamic simulations, parameter estimation, data reconciliation, sensitivity analysis, and optimization. Developers also implemented plugins that make possible the communication between EMSO and other software, e.g., thermodynamic databases[26].

In the present paper, an MPC scheme is proposed and implemented in a four-stage evaporator used in a sugarcane biorefinery that integrates the production of first- and second-generation ethanol. It is based on a feedforward neural network model of the system. The aim was to control sugar concentration at the outlet of the system. A phenomenological nonlinear dynamic model implemented in EMSO coupled with VRTherm, a thermodynamic plugin, represented the plant and provided the simulations to test the control system. Disturbances were applied on sugarcane juice temperature, juice volumetric flow rate, and juice sugar concentration simultaneously in pairs, and on the glucose syrup volumetric flow rate. The set-point was also changed for a servo performance test. These disturbances were applied to evaluate the control system performance in different situations, such as disturbance rejection and set-point tracking.

Methods

Phenomenological model for the multiple-stage evaporation system

A schematic representation of the evaporation system is presented in Fig. 1. The system model is a set of phenomenological equations of a quadruple-stage evaporator system. The layout is based on the infrastructure already established in many first-generation sugarcane ethanol plants in Brazil, with the usage of co-current four-stage evaporators.

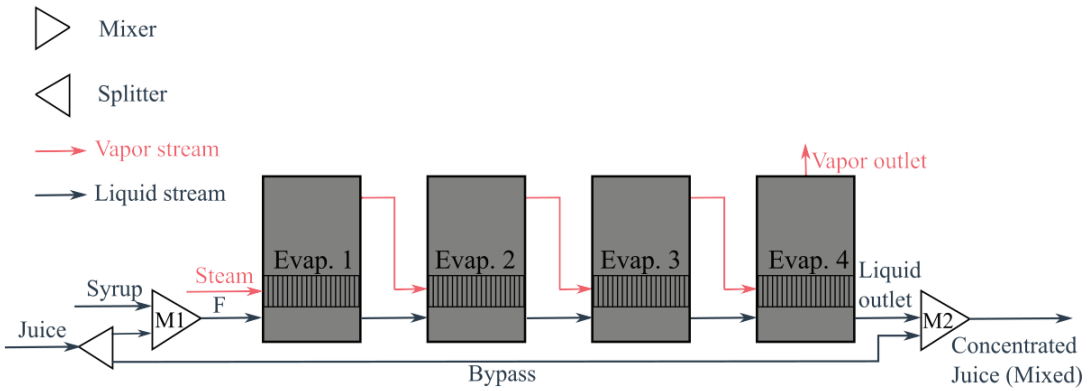

Fig. 1 – *Schematic representation of the evaporation system*

Each stage has steam and juice inlets, and liquid (concentrated juice) and steam (vegetal steam) outlets. Initially, clarified juice (*Juice* in Fig. 1), which represents juice after the stage of sugarcane milling and juice clarification, is split into two parts. One of these branches is mixed with the hexose syrup (*Syrup*) generated with the hydrolysis of the cellulose present in the sugarcane bagasse. The mixed juice is then used as a feed stream to the evaporators. The other branch (*Bypass*) is mixed with the concentrated juice outlet of the fourth evaporator (*Liquid outlet*) and sent to a buffer tank, which, in its turn, is responsible for providing the stream that feeds the fermentation system. Further detailed information about the model can be found in Emori *et al.*[27]

A stream of saturated steam at 405 K and 2.37 atm was used to feed the evaporator system. At 373 K and 2.3 atm, the clarified juice stream contained a 15-weight percent sucrose mixture in water. From the total of 650 $m^3\ h^{-1}$, 350 $m^3\ h^{-1}$ were bypassed. The evaporator feed stream was made by combining the not-bypassed stream with glucose syrup, which was then fed to the first stage of evaporation and concentrated to around 50 Brix degrees in the set of evaporators. After that, the bypassed juice stream was combined with the concentrated juice (*Liquid outlet*) to obtain the appropriate concentration for the fermentative process, 24.0 Brix degrees.

Based on one of the hypotheses of the study of Furlan *et al.*[28], the glucose syrup stream is taken to be a mixture of only water and glucose (10 wt%) at the same temperature and pressure of the clarified juice stream. The considered second-generation ethanol production process makes use of the Organosolv pretreatment process. After the pretreatment of bagasse, a filter separates the solid cellulose-rich stream from the liquid stream, which contains the hydrolyzed hemicellulose and solubilized lignin. The solid fraction is washed with NaOH aqueous solution to remove, in a second filter, the remaining lignin that eventually may be entrapped in the solids. Just after that, the cellulose fraction is hydrolyzed with specific enzymes to produce the glucose (hexose) syrup. Therefore, there are no other sugars in the glucose syrup sent to the evaporators.

Neural Network

In comparison with a phenomenological model, a black-box model acts as a faster substitute since it does not require solving a system of multiple differential-algebraic equations. Therefore, in order to obtain an internal model for the MPC, a feedforward artificial neural network with one input layer, one output layer, and one hidden layer was chosen to approximate the dynamic phenomenological model to a black-box model. The objective was to use the neural network to predict the second mixer (M2 in Fig. 1) outlet (*Concentrated Juice*) concentration response to disturbances in the feed juice (*Juice*) properties and glucose syrup (*Syrup*).The network was developed using the Scilab ATOMS open-source module named "Neural Network Module"[29].

The selected activation functions for the hidden layer and the output layer were tan-sigmoid and linear, respectively. The network architecture, illustrated in Fig. 2, was selected because this is the standard network for function approximation[30]. The scheme shows an input layer with u input values and hidden and output layers composed of nodes with W weights values and b bias values. This neural network was trained using a backpropagation scheme. The optimization routine chosen was the gradient descent, and a momentum training function was used with mean square error as the objective function. To avoid overfitting problems, the training algorithm was interrupted as the neural network error values stagnated.

The neural network training parameters were selected by trial and error, analyzing the best responses of the system. The selected values were a learning rate of 0.05, a maximum of 8000 epochs, a momentum rate of 0.09, and a performance goal

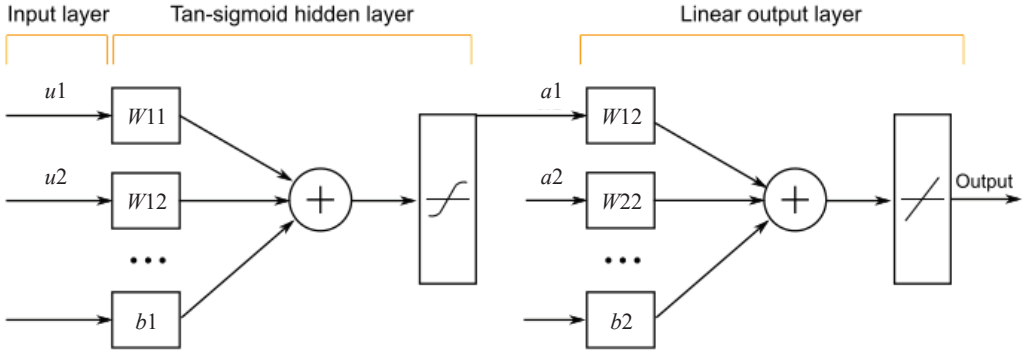

Fig. 2 – *Schematic representation of the neural network*

(minimum error) of 10^{-7}. The hidden layer was composed of 21 neurons. The number of neurons was selected based on an observable maximum increase in the learning capacity. When stagnation in the error reduction with the increase of the number of neurons was observed, then its amount was selected.

The output layer was composed of one neuron representing the prediction of the second mixer output juice concentration (*Concentrated Juice* stream in Fig. 1). Five variables were selected for the input layer based on the main variables that affect the dynamics of the output juice concentration: temperature, volumetric flow rate, and sugar concentration of the clarified juice stream (*Juice*), the first evaporator feed steam temperature, and the glucose syrup flow rate. As a model approximation procedure, the previous value predicted in the output layer was also used as a sixth input for the next prediction, generating a cascade effect.

Data generated from simulations of the phenomenological model were used as input information to the neural network. The training data was obtained by applying disturbances in the *Juice* and *Syrup* streams. All other variables were maintained unchanged. Therefore, the bypass fraction value was fixed, although the bypass stream characteristics changed as disturbances were applied. The second mixer outlet concentration was used as the outlet training variable of the neural network. This data was composed of an array of 5750 values for each input and output variable. For a better prediction capacity and compatibility with the MPC model requirements, all values were normalized in order to reach similar magnitudes. It is considered that the steady-state values were the initial ones. To generate the training input information, different step disturbances were applied to each input variable simultaneously using a sigmoid equation, shown in Equation (1).

$$X = X_0\left[\left(\frac{Pf}{1+e^{\tau_0-\tau}}\right)+1\right] \qquad (1)$$

In this equation, X_0 and X are the variable value at steady-state and after the disturbance, respectively. *Pf* is the fraction of variation that the disturbance magnitude represents relative to the variable steady-state value X_0. τ_0 represents the time in which the disturbance occurs (selected to be 600 seconds), and τ is the time of the simulation.

The disturbances were applied right after the start of the simulation simultaneously in the five input process variables of the neural network: temperature, volumetric flow rate, and sugar concentration of the clarified juice stream (*Juice*), the first evaporator feed steam temperature, and the glucose syrup flow rate. Twenty-three different simulations ran in EMSO, each for 12,500 seconds with steps of 50 seconds, generating a total of 5750 points. Another four similar simulations were run and used for validation purposes.

Model Predictive Control

An MPC scheme was developed to control the second mixer outlet sugar concentration. Since this stream is the system outlet, the scheme has the capacity to control the concentration of the entire system. Besides, MPC is effective against large dead response times that are present when control devices are inserted in the outlet of a multiple-stage evaporator. The manipulated variable was the steam flow rate fed to the first evaporator.

The MPC algorithm was also implemented in Scilab. It considers parameters that are related to its predictive and control capacity. The control horizon *M* defines how many control action steps are calculated in the prediction. The prediction horizon *P* defines of how many steps ahead the prediction will be made. The sampling instant *k* is present because this algorithm moves through the time at each sampling, developing its predictions based on past outputs and control actions, optimizing the future control action based on how far the predicted future output is from the set-point. Fig. 3 shows a schematic representation of an MPC.

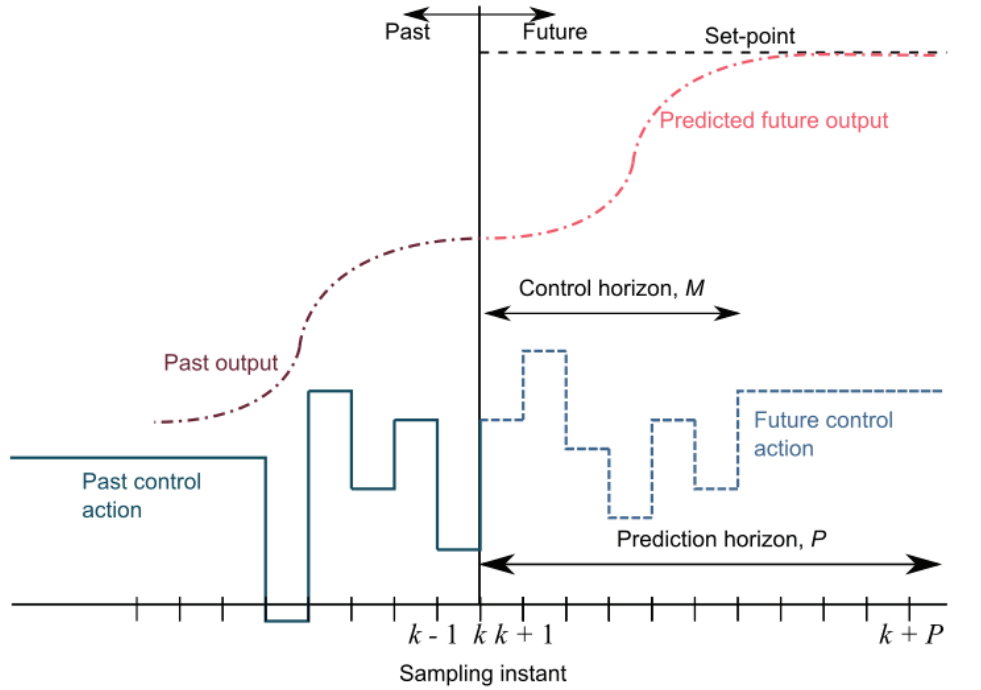

Fig. 3 – *Scheme of an MPC*

A Dynamic Matrix Control (DMC) was selected as the MPC scheme using an artificial neural network model. After the neural network training stage, step-response models were simulated in EMSO and then introduced into the MPC algorithm in the form of Equation (2). The main advantage of this approach is that step-response models can represent stable processes with unusual dynamic behavior that cannot be accurately described by simple transfer function models[23].

Equation (2) describes the step-response model of the second mixer outlet sugar concentration. In this equation, for each step k and future predicted step j, $y(k+j)$ is the sugar concentration at the $k+j$ sampling instant, $\Delta u(k-i+j)$ is the change in the manipulated variable from one sampling instant to the next, N is the number of S step-response coefficients (the magnitude of variation of the response to a step disturbance at each sampling i), and y_0 is the initial sugar concentration.

$$y(k+j) = y_0 + \sum_{i=1}^{N-1} S_i \Delta u(k-i+j) + S_N u(k-N+j) \quad (2)$$

The DMC algorithm is based on predictions of future outputs on a limited time interval, named prediction horizon. These predictions are also based on the step-response model and are calculated with Equation (3), in which $\hat{y}(k+j)$ represents the sugar concentration predicted value. The s values are the step-response coefficients calculated through the neural network model in each step k.

$$\hat{y}(k+j) = \sum_{i=1}^{N-1} s_i \Delta u(k-i+j) + s_N u(k-N+j) \quad (3)$$

Equation (3) terms can be expanded and divided into past and future control actions, as shown by Equation (4). The first sum expression denotes the effect of future control moves, and the second denotes the effect of past control moves.

$$\hat{y}(k+j) = \sum_{i=1}^{j} s_i \Delta u(k-i+j) + \sum_{i=j+1}^{N-1} s_i \Delta u(k-i+j) + s_N u(k-N+j) \quad (4)$$

A bias correction is added to the prediction based on the difference between the predicted response and the real response (from EMSO step-response model). The corrected prediction is obtained through Equation (5), in which $\tilde{y}(k+1)$ represents the sugar concentration corrected prediction value.

$$\tilde{y}(k+1) = \hat{y}(k+1) + \left[y(k) - \hat{y}(k) \right] \quad (5)$$

When substituting Equation (4) into Equation (5) and writing it in matrix form, Equation (6) is obtained. S_f and S_{past} are the vector of future and past step-model coefficients, respectively, Δu_f and Δu_{past} are the vectors of future (represented by the f subscript) and past control moves (represented by the *past* subscript), respectively, and d is the error vector that denotes the difference between the predicted and the correct model.

$$\tilde{Y} = S_f \Delta u_f + S_{past} \Delta u_{past} + s_N u_{past} + d \quad (6)$$

The difference between the past control effect and the set-point is denominated unforced error E,

and is given by Equation (7). It represents the distance between the set-point and the controlled variable if no future control moves are applied.

$$E = S_{past}\Delta u_{past} + s_N u_{past} + d \tag{7}$$

The DMC control law is based on the minimization of the objective function represented by Equation (8). P is the prediction horizon, r_{k+1} is the control set-point at each i sampling, w is the control weight coefficient that limits the magnitude of the control actions, and M is the control horizon.

$$\varphi = \sum_{i=1}^{P}\left(r_{k+1} - \tilde{y}_{k+1}\right)^2 + w\sum_{i=0}^{M-1}\left(\Delta u_{k+1}\right)^2 \tag{8}$$

The MPC control law that minimizes this objective function is obtained from its derivative with respect to Δu. By setting this derivative to zero, Equation (9) is obtained. ${S_f}^T$ is the transpose of the vector S_f, and W is the vector of control weight coefficients.

$$\Delta u_f = \left({S_f}^T S_f + W\right)^{-1} S_f E \tag{9}$$

Control system

The MPC scheme was coupled in a closed-loop system based on the work of Emori *et al*. It consists of PI level controllers on all evaporators and PI pressure controllers in the second, third, and fourth stages to prevent high oscillations in the multiple-stage evaporator response, and to prevent high variations in each valve opening input due to the system response to disturbances. This type of controller is usually applied for pressure and level control with the derivative term discarded. Both PI controllers manipulate an outlet valve opening fraction. The liquid outlet stream flow rate is used to control the level, whereas the vegetal steam outlet flow rate is used to control the pressure. More details can be found in Emori *et al*.[27]

For comparison purposes, tests were made with a PID concentration controller using the same controlled (second mixer outlet sugar concentration) and manipulated (steam flow rate fed to the first evaporator) variables of the MPC scheme.

The controller parameters were based on the values used by Emori *et al*.[27] However, the scheme was changed by the addition of a PI temperature controller in the second stage and, differently from Emori *et al.*, the second mixer outlet stream concentration was controlled, instead of the fourth stage liquid outlet concentration. This approach is more general and also takes the bypass stream into account. Therefore, the system dynamics changed and new parameters were calculated for these components. The tuning method used was the same as in the cited work. The second stage PI temperature controller was configured with a proportional gain of 7.0 and an integral time of 1.8 min. The PID concentration controller was configured with a proportional gain of 0.178, an integral time of 62.9 s, a derivative time of 15.2 min, and a set-point of 24.0 Brix degrees (the same set-point value of the MPC).

Simulation

The simulation was carried out in EMSO process simulator using SUNDIALS as a differential and algebraic equation solver algorithm. The application of step disturbances in the simulation was introduced through a sigmoid equation (Equation (1)).

With the purpose of calculating the thermodynamic properties of mixtures and compounds, the VRTherm thermodynamic database was used along with the EMSO library of properties. This software uses empirical correlations and state equations as functions of state variables to obtain these properties. More details can be found in Emori *et al.*[27]

Results and discussion

Neural Network Model

Fig. 4 shows the best results of the neural network model with the momentum training function. The graph shows the response of the sugar mass concentration of the second mixer outlet to disturbances in the form of Equation (1). These results were obtained after 8000 epochs, reaching mean square errors of $2.0\cdot10^{-5}$. Adaptive learning methods were also applied. However, it showed an unstable training stage and was discarded. The network presented a mean node weight value of 0.0012960 and a mean bias value of 0.0079388.

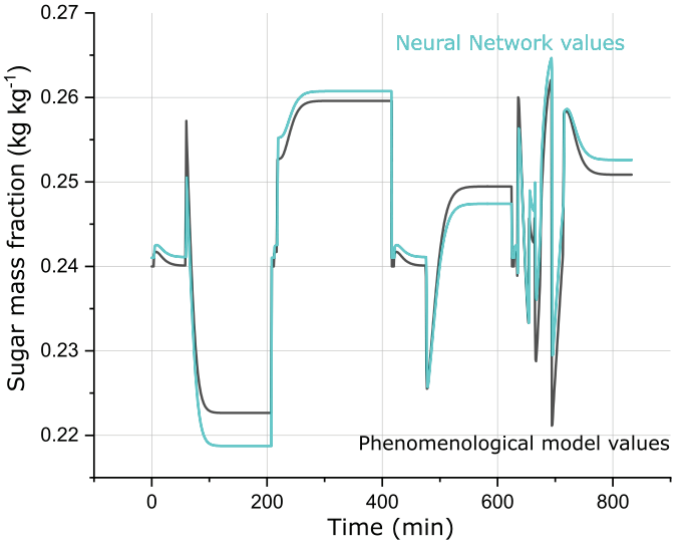

Fig. 4 – *Neural network performance in comparison with values generated by the phenomenological model*

For validation purposes, the figure shows the values generated by the neural network using data from four simulations that were not used in the training stage. As can be seen, the neural network demonstrated an efficient performance, with adequate generalization and capacity to reproduce the phenomenological model dynamic behavior.

Set-point tracking

To evaluate changes in the product specifications, a set-point tracking problem was approached. Therefore, a servo problem of a set-point step increase of 3.0 Brix degrees was applied in the concentration controller of the second mixer outlet, resulting in a change of sugar mass fraction from 0.24 to 0.27. The tests were made with different MPC parameters, and the best results regarding settling time and overshoot value were reached with a control horizon M of 5, prediction horizon P of 15, and a weight factor w of 0.0005.

Fig. 5 presents results for the servo problem, i.e., the response of the control system to the change in the set-point. Although there is a gap between the neural network prediction and the phenomenological plant model, the bias correction shown in Equation (5) mitigated this problem, and the servo problem was successfully addressed. This difference can be explained by the nonlinearity of the multiple-stage evaporator system and the error present in the neural network model.

Fig. 5b shows the behavior of the PID and the MPC concentration controller to the same set-point step change. It can be seen that both achieved the new set-point; however, due to the long delay and dead-time responses of the evaporator system, the classical controller took a longer time to reach the set-point value, with a settling time of about 120 minutes compared to 60 minutes of the MPC. Although the MPC presented a better performance, both control schemes were satisfactory in set-point tracking changes. The performance can be compa-

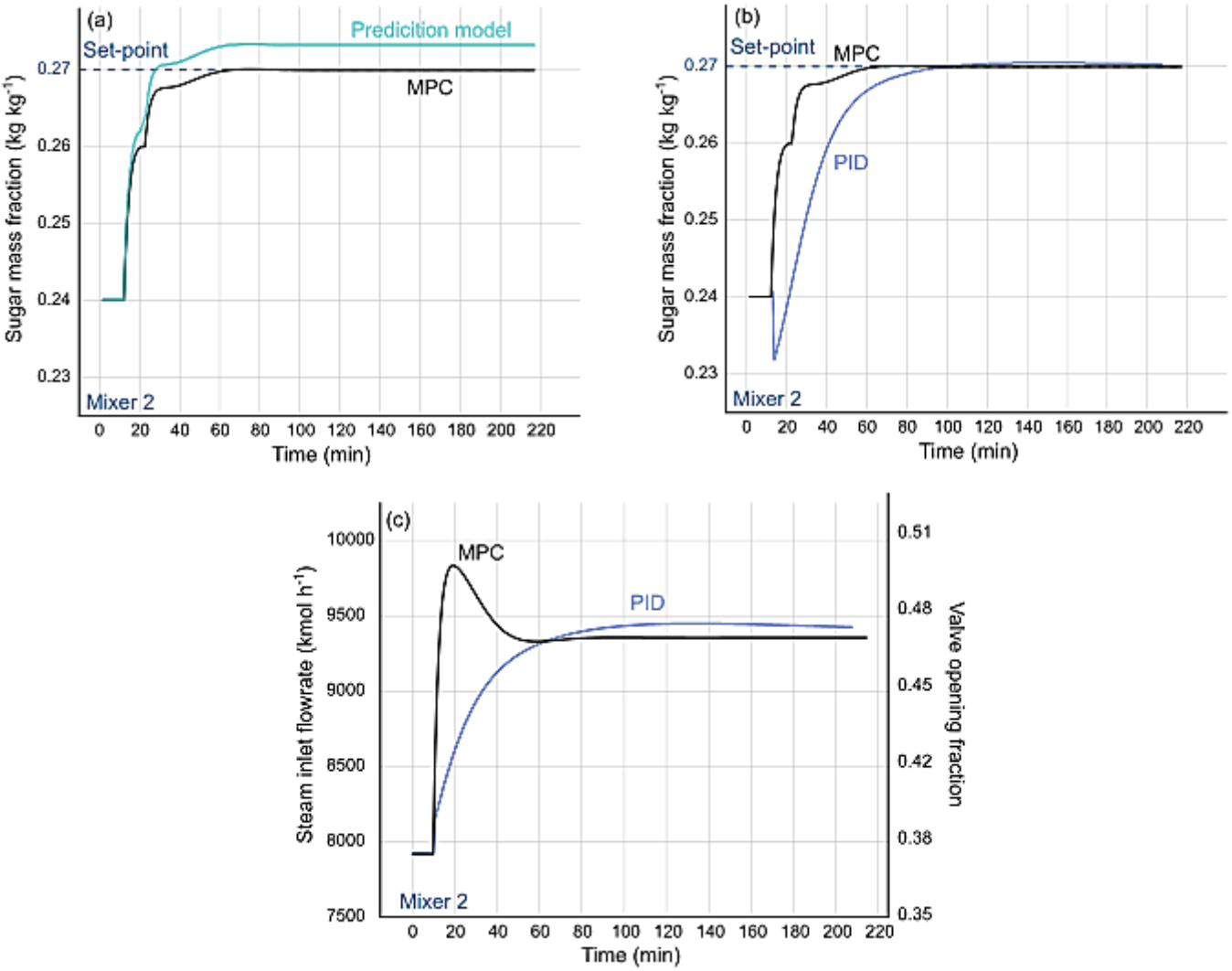

Fig. 5 – *MPC response on the plant model (EMSO model) and prediction model (a), comparison of the MPC and the PID performance (b), and manipulated steam flow rate and valve opening behavior (c) to an increase of 3.0 Brix in the set-point*

red qualitatively and timewise quantitatively with the work of Razzanelli *et al.*[31] with an application of MPC in a four-stage evaporation unit with concentration set-point changes. In that study, the best results showed settling times ranging from 60 to 90 minutes.

From the manipulated variable graph, it can be observed that, although both schemes reached the same set-point, the manipulated variable reached different states. The expected MPC faster response can be observed as it applies a more intense initial response when compared with the PID trajectory.

Disturbance rejection

To demonstrate its effectiveness against disturbances, the proposed MPC scheme was tested by applying step disturbances in properties of the sugarcane juice stream that commonly affect the evaporator performance: a step increase in the sucrose mass percentage of the clarified juice (Brix degree) by 2 points, increasing its concentration from 15 to 17 °Brix; a step increase in the volumetric flow rate of the clarified juice in 10 % of its steady-state value (650 $m^3\ h^{-1}$); and a step raise in the clarified juice temperature of 5 K. These disturbances were applied simultaneously in pairs, simulating possible changes in these variables caused by feedstock and operating random variations that are usually present in an industrial process. A disturbance was also applied to the glucose syrup volumetric flow rate, decreasing its value by 30 % and 45 %. As in the set-point tracking tests, a control horizon M of 5, a prediction horizon P of 15, and a weight factor w of 0.0005 showed to be the best MPC parameters for disturbance rejection.

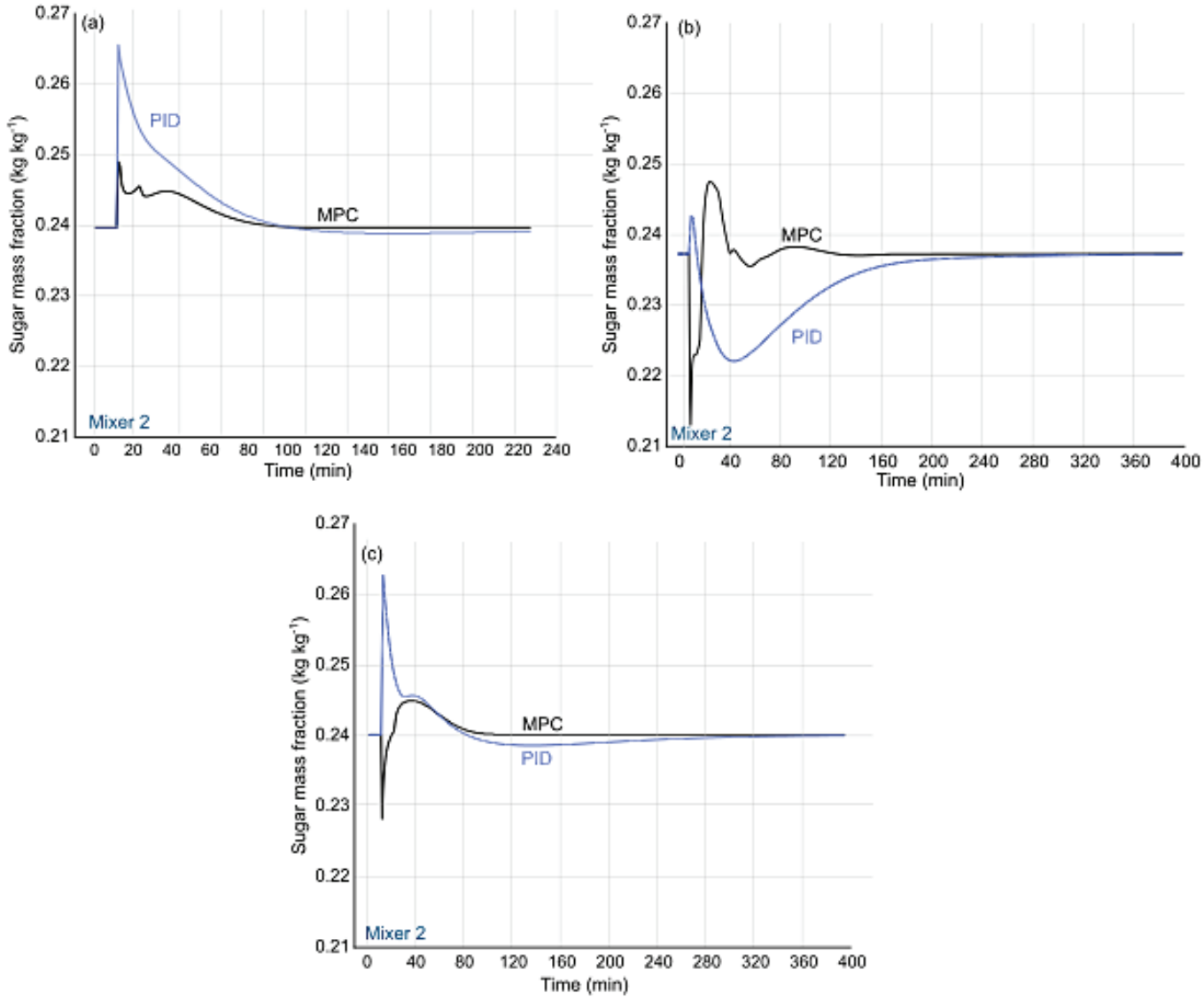

Fig. 6 – *Responses of MPC and PID controlled evaporators on the second mixer to simultaneous step disturbances in juice sugar concentration and temperature (a), juice volumetric flow rate and temperature (b), and juice sugar concentration and volumetric flow rate (c)*

The MPC response to the disturbances in the sugarcane juice stream is presented in Fig. 6. The graph shows the sugar mass fraction of the outlet of the second mixer to simultaneous disturbances on the juice concentration and temperature (Fig. 6a), juice volumetric flow rate and temperature (Fig. 6b), and juice concentration and volumetric flow rate (Fig. 6c). Also, as a means of comparison, the response of the PID concentration controller for the same set of disturbances is shown. From the figure, although both successfully reached the set-point value, it can be seen that the MPC scheme performs better than the PID controller regarding the settling time. An initial overshoot can be seen in both control scheme responses, but it is rapidly decreased as the control action is applied. This sudden change is generated by the bypass parameter values variations due to the disturbances. Since the bypass fraction is constant and this stream heads directly into the second mixer, any variation in the flow rate of the juice is driven both to the set of evaporator stages and the outlet mixer; furthermore, the sudden change in temperature or concentration is also present in the bypass stream, leading to an overshoot in the early moments after the disturbances are applied. The different behavior, after the early moments, is attributed, then, to the different control actions generated by the PID and MPC controllers. As a consequence, these distinctive actions lead to different states and control actions in the level and pressure PI controllers. It is interesting to observe also that the simultaneous volumetric flow rate and temperature disturbances generated the response with the highest variation. It can be explained by the fact that, along with the concentration disturbance, a flow rate change affects the system less as these two disturbances present opposite effects on the outlet concentration. However, being applied with the temperature disturbance, an increase in the evaporator feed flow rate results in a higher decrease in the juice concentration.

The behavior of the manipulated steam inlet flow rate fed to the first evaporator when disturbances in the sugarcane juice stream occurred can be seen in Fig. 7. The same scale was used in the three graphs of Fig. 7 for comparison purposes. The fast settling time provided by the MPC scheme is possible due to rapid variations in the feed steam valve opening. However, a high variation as the one observed in Fig. 7b (which is closely related to the fact that this pair of disturbances leads to the highest variation in the controlled variable response) may cause deterioration in the valve structure. Therefore, in the case of strong disturbances, an increase in the control weight coefficient in Equation 8 may be necessary to adequate the intensity of the control action to this disturbance.

The 30 % decrease in the glucose syrup volumetric flow rate was well handled by both control schemes, as can be seen in Figs. 8a and 8b. The MPC performance presented a lower settling time, but with a higher variation on the manipulated variable. In the case of a disturbance of higher magnitude, more intense variations on steam flow rate are necessary, as can be seen in Figs. 8c and 8d. This time, a 45 % decrease was applied in the syrup flow rate. It is possible to see that the PID is reaching its stability limits. However, the MPC was still able to bring back the controlled variable to the set-point with no trouble. It shows not only faster responses but also more robustness than the classical control.

In comparison with the other disturbances, this response had a higher settling time for the MPC due to the increased magnitude of the step value. For this reason, it may be necessary to decrease the value of the weight factor parameter, although it may increase the overshoot value. With a lower weight factor, the MPC can apply control actions with the necessary higher intensity to handle the magnitude of the glucose syrup disturbance. Therefore, it is interesting to input a simple change in the weight factor parameter when changes of high magnitude in the flow rate are necessary. It may occur when a problem is detected or deactivation is necessary in the glucose syrup production stage. The implementation of this scheme is simple since it requires only a flow rate measurement, which is easily done.

In both feed juice and glucose syrup disturbance tests, the manipulated variable presented different behavior for PID control and MPC. With different stationary settling values, it demonstrates that the nonlinearity of the multiple-stage evaporation system can affect the control performance. Both schemes work with the error, *i.e.*, the difference between the set-point and the controlled variable. However, it is clear that the manipulated variable trajectory is highly different for both schemes, and is the factor that makes the MPC superior to the PID.

Table 1 shows the metrics of the MPC and PID performances as a means of comparison. These metrics are the settling time, mean square error (MSE) from the set-point value (measured from the sugar mass fraction), and the highest variation value in the sugar mass fraction. In general, the MPC performed better, particularly concerning the settling time. This fact is expected, since the main feature of the MPC is its prediction capacity, leading to a faster response. Also, the MPC performance presented better mean square error values. The results in Table 1 show that, in the disturbance tests for both sugarcane juice and glucose syrup flow rates, the MPC responses were superior. In comparison with the PID, the MPC settling times were 43.0 % faster on

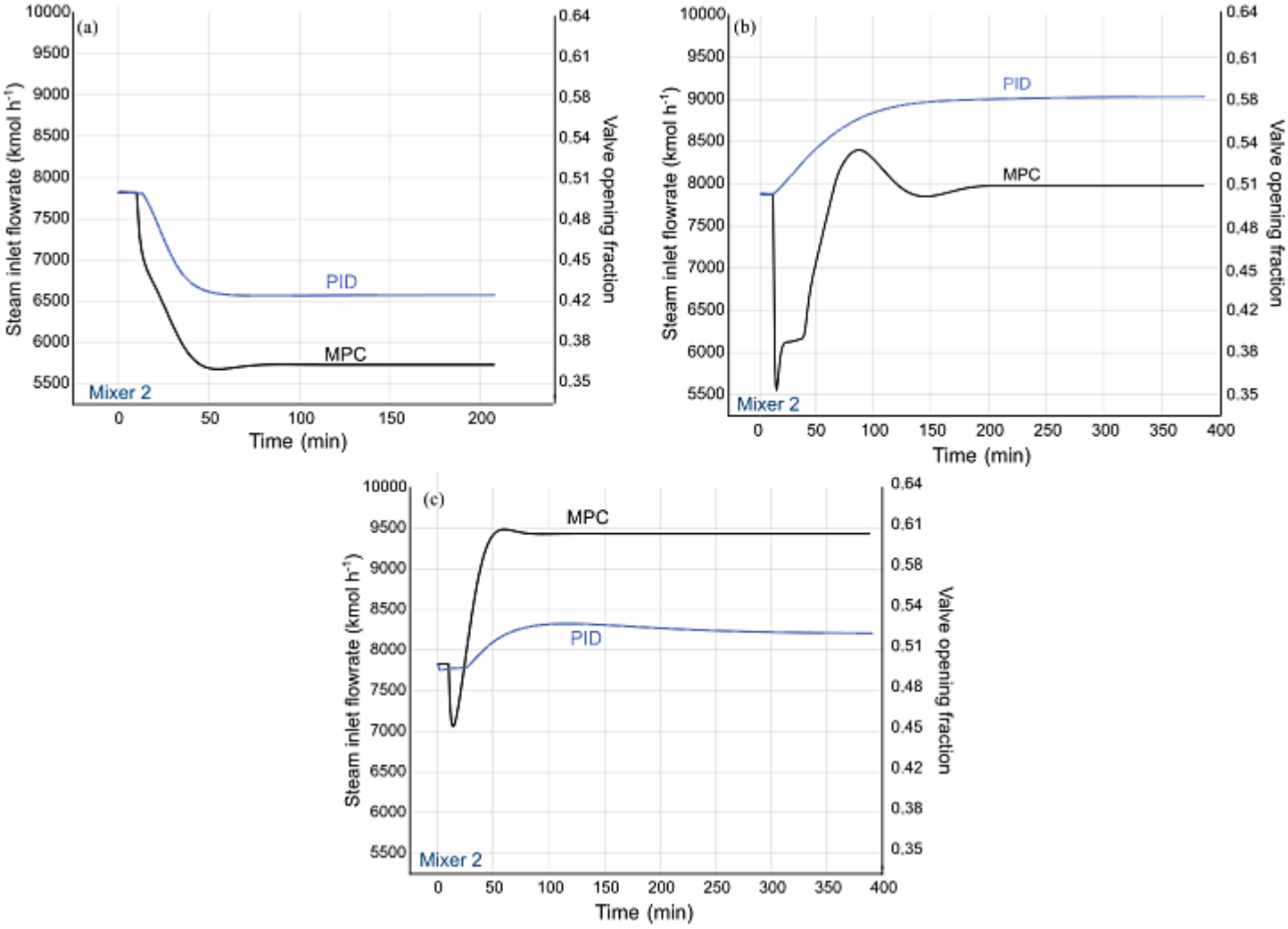

Fig. 7 – *Manipulated valve opening and steam inlet flow rate fed to the first effect when simultaneous disturbances in juice sugar concentration and temperature (a), juice volumetric flow rate and temperature (b), and juice sugar concentration and volumetric flow rate (c) are applied*

Table 1 – *Control metrics related to the response of MPC and PID controllers to different disturbances. The controlled variable is the concentration of the concentrated juice that leaves the system, and the manipulated variable is the flow rate of steam fed to the first effect.*

Disturbances	Settling time (min)		MSE		Absolute Highest variation	
	MPC	PID	MPC	PID	MPC	PID
Juice concentration and temperature	82	93	$4.88 \cdot 10^{-6}$	$3.21 \cdot 10^{-5}$	0.009	0.025
Juice flow rate and temperature	132	173	$2.61 \cdot 10^{-5}$	$8.05 \cdot 10^{-5}$	0.027	0.018
Juice concentration and flow rate	110	349	$4.89 \cdot 10^{-6}$	$5.61 \cdot 10^{-5}$	0.012	0.022
Glucose syrup flow rate (–30 %)	190	355	$5.07 \cdot 10^{-5}$	$7.49 \cdot 10^{-5}$	0.031	0.018
Glucose syrup flow rate (–45 %)	183	450	$8.46 \cdot 10^{-5}$	$1.95 \cdot 10^{-4}$	0.046	0.034

average. The table also shows an average reduction in mean square error of 63.5 % with the predictive controllers. In comparison with the recent literature, a study with step-change disturbance tests performed on a four-stage evaporator showed a reduction of 53.34 % in the mean square error[32]. Although the MPC was applied in a different process, the performances can be compared since the evaporation unit is similar and the authors also applied neural network MPC control.

Tests were also made by changing the operating conditions. To simulate possible changes in

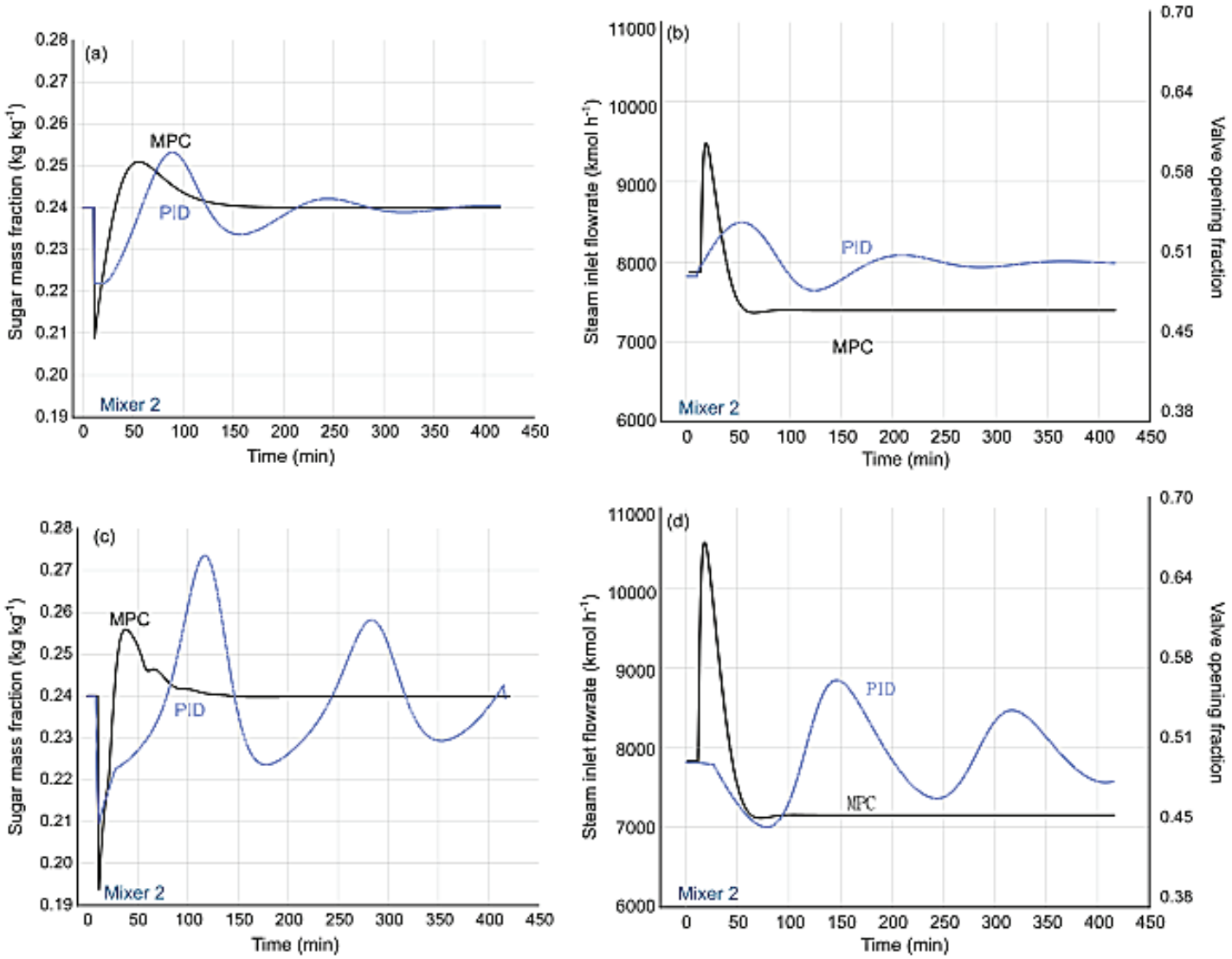

Fig. 8 – *Responses of MPC and PID controlled concentration on the second mixer to a step disturbance in the glucose syrup volumetric flow rate of –30 % (a) and –45 % (c), and behavior of the manipulated valve opening and steam inlet flow rate fed to the first evaporator (b) and (d) for –30 % and –45 %, respectively*

feedstock intake, a disturbance rejection test was applied in a scenario with an initial positive and negative change of 30 % in the juice volumetric flow rate in comparison with the nominal value of 650 $m^3\ h^{-1}$ used before. The steam initial flow rate was also changed accordingly to maintain the mixer outlet concentration initially at 24.0 °Brix. A simultaneous step increase in concentration and temperature similar to the one applied in the previous disturbance rejection test was applied with the different initial conditions. The main issue with changing significantly the juice flow rate is that it changes the interaction between the steam flow rate and the concentration. Therefore, the neural network must be able to generalize these changes accordingly.

Fig. 9a shows the MPC performance within these different scenarios. As a means of comparison, the MPC response for these disturbances in the nominal operating configuration is also displayed. The figure shows that the MPC was able to handle the disturbances in all situations. As expected, a lower juice flow rate presented an initial higher overshoot but required less variation in the steam usage since the amount of liquid was also lower. The opposite occurred with an increased juice flow rate. Therefore, this test showed the capability of the MPC and the neural network to work in different scenarios that would render the classical PID inefficient. Fig. 9b depicts the variation in steam flow rate (and in the valve opening fraction) caused by the disturbances used in each scenario. The initial response of the system in all cases showed an increase in the outlet juice concentration. Consequently, as expected, the MPC applied negative steam flow rate variations, to decrease the juice concentration and reach the set-point, as can be seen in Fig. 9b.

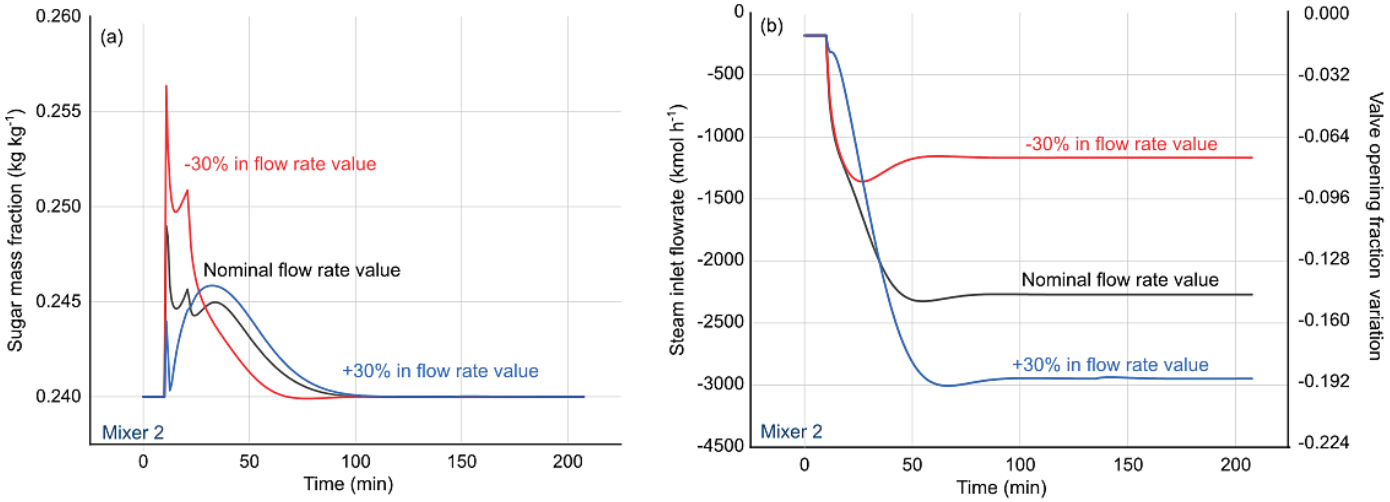

Fig. 9 – *Responses of MPC controlled concentration on the second mixer to simultaneous disturbances in juice sugar concentration and temperature (a) and behavior of the manipulated valve opening and steam inlet flow rate fed to the first evaporator (b) for different values of juice flow rate*

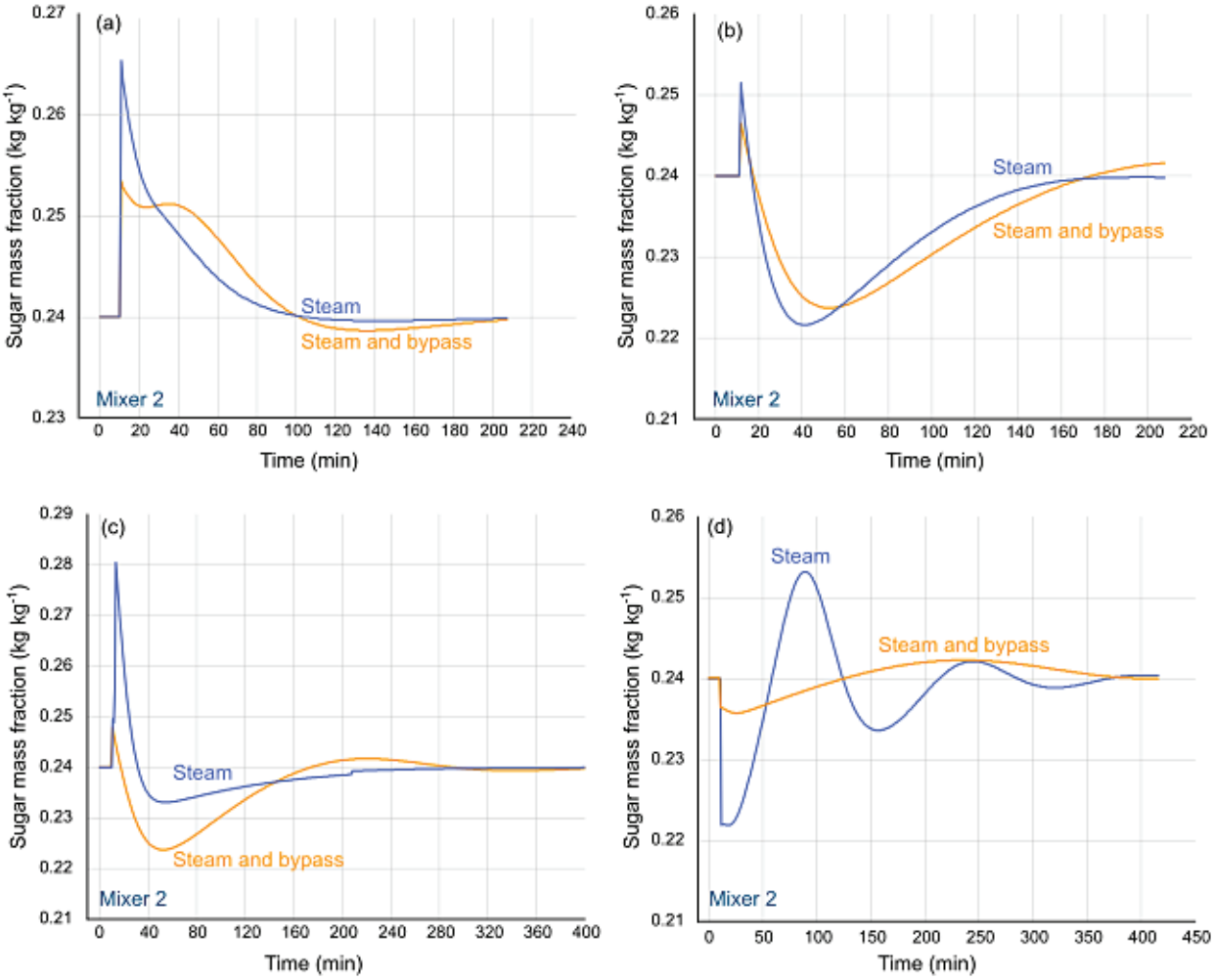

Fig. 10 – *Responses of two different strategies for controlling the concentration of the output of the second mixer to simultaneous step disturbances in juice sugar concentration and temperature (a), juice volumetric flow rate and temperature (b), juice sugar concentration, and volumetric flow rate (c), and a 30 % step disturbance in the glucose syrup volumetric flow rate (d). The strategies are PID controller manipulating steam flow rate fed to the first effect and the same PID controller coupled to a PI controller manipulating splitter fraction value.*

Although being able to handle the disturbances, this control scheme (*i.e.*, control of the concentration of the concentrated juice that leaves the system by manipulating flow rate of steam fed to the first stage) showed limitations regarding disturbances of higher magnitude. Fig. 8 shows that the PID controller generated oscillations, suggesting a change in the gain value. However, these changes can affect negatively the responses to other disturbances.

The main reason for this limitation is the fact that this control scheme affects only one of the two inputs to mixer M2. Therefore, changing its concentration will only change the mixer output concentration to a certain level. One solution to this problem could be coupling a second controller that manipulates the fraction of the clarified juice sent to the bypass. The main objective of this strategy is to aid the first concentration controller in the presence of disturbances of higher magnitude. In this context, a PI concentration controller was inserted to manipulate this fraction, controlling the concentration of the second mixer output simultaneously with the steam manipulator controller. However, changes in the bypass fraction can affect the first controller action performance. Therefore, a low gain value of the PI concentration controller was set as a means to generate significant control action only in a relatively high concentration value deviation from the set-point. The tuning method was the same as that of the other classical controllers, with a proportional gain of 0.011 and an integral time of 1.3 min.

An improvement can be seen in Fig. 10, which shows a comparison between the first control strategy (PID controller manipulating steam flow rate) and the second one (PID controller manipulating steam flow rate coupled with the PI controller manipulating splitter fraction to bypass stream). Although slightly increasing the settling time of the simultaneous disturbances, this change showed a significant impact on the glucose syrup flow rate disturbance response, decreasing the oscillation and the overshoot. The main advantage of this control system is to overcome the magnitude limit of the disturbance rejections. Therefore, it can be useful in situations where failures are presented by the lignocellulosic material processing or even in the case of changes in the operating parameters. Tests were also performed with the coupling of the MPC controller to the PI controller manipulating the splitter fraction to the bypass stream. However, no significant changes were presented. Although not presenting significant changes, the MPC performance was still superior in comparison with the PID.

Conclusions

In the present paper, a dynamic phenomenological model of a quadruple-stage evaporation system used in the integrated first- and second-generation ethanol production in sugarcane autonomous biorefineries was used to train a feedforward artificial neural network. The objective was to obtain a black-box model to use as an internal prediction model for an MPC scheme. The non-commercial process simulator EMSO was used to model, simulate, and generate transient responses of the evaporation system to be used as training and validation data. The neural network and the MPC scheme were implemented in Scilab to control the outlet juice concentration of the evaporation system.

A neural network topology was selected and a backpropagation scheme with gradient descent and a momentum training function with a mean square error as the objective function was used. The trained network showed good generalization and efficiency to approximate the model dynamics.

In both servo and regulatory problems, the MPC implemented in parallel with PI pressure and level controllers showed good results as it was able to quickly track new set-points and mitigate disturbances. The advantage of this scheme, mainly in the settling time and robustness, became evident when comparing the closed-loop responses to those of a classical PID controller in parallel with PI pressure and level controllers when applying the same inputs. Therefore, the proposed advanced controller showed to be more suitable to control this type of system. The results also showed that the coupling of the PID controller to a PI controller that manipulated the bypass splitter fraction value enhanced the control system flexibility, enabling the rejection of disturbances of higher magnitudes, and facilitating changes in operating parameters that may be necessary.

ACKNOWLEDGMENTS

The authors acknowledge the National Council for Scientific and Technological Development – CNPq (Brazil), processes 311807/2018-6, 428650/2018-0, 140127/2020-8, 307958/2021-3, and Coordination for the Improvement of Higher Education Personnel – CAPES (Brazil) for the financial support.

List of simbols

d	– subscript for the difference between the predicted and the correct sugar mass fraction
E	– subscript for the difference between the past control effect and the set-point
f	– subscript for variables of future steps
i	– counter for each step
j	– counter for each future step

k – subscript for the current step
M – control horizon
N – total number of steps
r – sugar mass fraction set-point
s – neural network calculated step magnitude
S – step response magnitude
S_f – vector of future step coefficients
S_{past} – vector of past step coefficients
u – size of change in the manipulated variable, mol h^{-1}
u_{past} – size of change already applied in the manipulated variable, mol h^{-1}
w – manipulated variable weight coefficient
W – vector of manipulated variable weight coefficient
y – sugar mass fraction
y_0 – initial sugar mass fraction
$\tilde{y}$ – corrected sugar mass fraction prediction
$\hat{y}$ – predicted sugar mass fraction
$\tilde{Y}$ – vector of corrected sugar mass fraction prediction
φ – objective function

References

1. *Cortes-Rodríguez*, *E. F.*, *Fukushima*, *N. A.*, *Palacios-Bereche*, *R.*, *Ensinas*, *A. V.*, *Nebra*, *S. A.*, Vinasse concentration and juice evaporation system integrated to the conventional ethanol production process from sugarcane – Heat integration and impacts in cogeneration system, Renew. Energy **115** (2018) 474. doi: https://doi.org/10.1016/j.renene.2017.08.036
2. Novacana. Lista de Usinas de Açúcar e Etanol do Brasil por estado. https://www.novacana.com/usinas_brasil/estados/ (In Portuguese)
3. UNICA – União da Agroindústria Canavieira de São Paulo. Moagem de cana-de-açúcar e produção de açúcar e etanol – safra 2019/2020. https://observatoriodacana.com.br/ (In Portuguese)
4. Carpio, *L. G. T., Simone de Souza, F.*, Optimal allocation of sugarcane bagasse for producing bioelectricity and second generation ethanol in Brazil: Scenarios of cost reductions, Renew. Energ **111** (2017) 771. doi: https://doi.org/10.1016/j.renene.2017.05.015
5. *Cubas-Cano*, *E., López-Gómez, J. P., González-Fernández*, *C., Ballesteros*, *I., Tomás-Pejó*, *E.*, Towards sequential bioethanol and L-lactic acid co-generation: Improving xylose conversion to L-lactic acid in presence of lignocellulosic ethanol with an evolved *Bacillus coagulans*, Renew. Energy **153** (2020) 759. doi: https://doi.org/10.1016/j.renene.2020.02.066
6. *Dias, M .O. S., Junqueira, T. L., Cavalett, O., Cunha, M. P., Jesus, C. D. F., Rossell, C. E. V., Maciel Filho, R., Bonomi, A*. Integrated versus stand-alone second generation ethanol production from sugarcane bagasse and trash, Bioresour. Technol. **103** (2012) 152. doi: https://doi.org/10.1016/j.biortech.2011.09.120
7. *Madaeni, S. S., Zereshki, S.*, Energy consumption for sugar manufacturing. Part I: Evaporation versus reverse osmosis, Energy Convers. Manag. **51** (2010) 1270. doi: https://doi.org/10.1016/j.enconman.2010.01.002
8. *Pazhany, A. S., Henry, R. J.*, Genetic modification of biomass to alter lignin content and structure, Ind. Eng. Chem. Res. **58** (2019) 16190. doi: https://doi.org/10.1021/acs.iecr.9b01163
9. *Wang, X., Li, C., Chen, X.*, Disturbance rejection control for multiple-effect falling-film evaporator based on disturbance observer, Trans. Inst. Meas. **38** (2016) 773. doi: https://doi.org/10.1177/0142331215597296
10. *Sousa, F. M. M., Fonseca, R. R.*, Application of adaptive feedforward-feedback control on multiple effect evaporator process, Chem. Prod. Process. Model. **14** (2019) 1. doi: https://doi.org/10.1515/cppm-2018-0040
11. *Adams, G. J., Burke, B. J., Goodwin, G. C., Gravdahl, J. T., Peirce, R. D., Rojas, A. J.*, Managing steam and concentration disturbances in multi-effect evaporators via nonlinear modelling and control, IFAC **41** (2008). doi: https://doi.org/10.3182/20080706-5-kr-1001.02356
12. *Pérez, L., Rodríguez, M. A., Fernández, F.,* Modelación matemática y simulación del control automático para el quíntuple efecto de evaporación del central azucarero "el palmar" en venezuela, Centro Azúcar **42** (2015) 48. http://scielo.sld.cu/pdf/caz/v42n2/caz06215.pdf
13. *Ahammad, S. H., Misra, Y., Bojja, P.*, A review of application of fuzzy controller in sugar industry, JARDCS **2** (2017) 34.
14. *Merino, A., Acebes, L. F., Alves, R., de Prada, C.*, Real time optimization for steam management in an evaporation section, Control Eng. Pract. **79** (2018) 91. doi: https://doi.org/10.1016/j.conengprac.2018.07.010
15. *Klaučo, M., Kalúz, M., Kvasnica, M.,* Machine learning-based warm starting of active set methods in embedded model predictive control, Eng. Appl. Artif. Intell. **77** (2019) 1. doi: https://doi.org/10.1016/j.engappai.2018.09.014
16. *Santos, J. E. W., Trierweiler, J. O., Farenzena, M.*, Model update based on transient measurements for model predictive control and hybrid real-time optimization, Ind. Eng. Chem. Res. **60** (2021) 3056. doi: https://doi.org/10.1021/acs.iecr.1c00212
17. *Smith, P. D., Swartz, C. L. E., Harrison, S. T. L.*, Control and optimization of a multiple effect evaporator, Proc. S. Afr. Sug. Technol. Ass. **74** (2000) 274.
18. *Benne, M., Grondin- Perez, B., Chabriat, J. P., Hervé, P.*, Artificial neural networks for modelling and predictive control of an industrial evaporation process, J. Food Eng. **46** (2000) 227. doi: https://doi.org/10.1016/S0260-8774(00)00055-8
19. *Ipanaque, W., Oliden, J., Manrique, J., Hernandez, A., Dutta, A., De Keyser, R.*, Nonlinear predictive control of an evaporator for bioethanol production, ECC **2013** (2013) 2573. doi: https://doi.org/10.23919/ecc.2013.6669595
20. *Acebes, L. F., Merino, A., Rodriguez, A., Mazaeda, R., de Prada, C.*, Model based online scheduling of concurrent and equal batch process units: Sugar end industrial case study, J. Process Control **80** (2019) 1. doi: https://doi.org/10.1016/j.jprocont.2019.05.005
21. *Mazaeda, R., Cristea, S. P., de Prada, C.*, Hierarchically coordinated economic MPC plantwide control of mixed continuous-batch units in process industries with application to a beet sugar plant, Optim. Control Appl. Methods **41** (2020) 190. doi: https://doi.org/10.1002/oca.2535

22. *Reese, B. M., Collins, E. G.*, A graph search and neural network approach to adaptive nonlinear model predictive control, Eng. Appl. Artif. Intell. **55** (2016) 250. doi: https://doi.org/10.1016/j.engappai.2016.07.00
23. *Afram, A., Janabi-Sharifi, F., Fung, A. S., Raahemifar, K.,* Artificial neural network (ANN) based model predictive control (MPC) and optimization of HVAC systems: A state of the art review and case study of a residential HVAC system, Energy Build. **141** (2017) 96. doi: https://doi.org/10.1016/j.enbuild.2017.02.012
24. *Tian, Y., He, Y. L., Zhu, Q. X.*, Soft sensor development using improved whale optimization and regularization-based functional link neural network, Ind. Eng. Chem. Res. **59** (2020) 19361. doi: https://doi.org/10.1021/acs.iecr.0c03839
25. *Klopot, T., Skupin, P., Metzger, M., Grelewicz, P.*, Tuning strategy for dynamic matrix control with reduced horizons, ISA Trans. **76** (2018) 145. doi: https://doi.org/10.1016/j.isatra.2018.03.003
26. *Henrique, J. P., de Sousa, R., Secchi, A. R., Ravagnani, M. A. S. S., Costa, C. B. B.*, Optimization of chemical engineering problems with EMSO software, Comput. Appl. Eng. Educ. **26** (2018) 141. doi: https://doi.org/10.1002/cae.21867
27. *Emori, E. Y., Ferreira, J., Secchi, A. R., Ravagnani, M. A. S. S., Costa, C. B. B.,* Dynamic study of the evaporation stage of an integrated first and second generation ethanol sugarcane biorefinery using EMSO software, Chem. Eng. Res. Des. **153** (2020) 613. doi: https://doi.org/10.1016/j.cherd.2019.11.002
28. *Furlan, F. F., Costa, C. B. B., Fonseca, G. de C., Soares, R. de P., Secchi, A. R., da Cruz, A. J. G., Giordano, R. de C.,* Assessing the production of first and second generation bioethanol from sugarcane through the integration of global optimization and process detailed modeling, Comput. Chem. Eng. **43** (2012) 1. doi: https://doi.org/10.1016/j.compchemeng.2012.04.002
29. *Luh, T. C.*, Neural Network Module. Published 2020. https://atoms.scilab.org/toolboxes/neuralnetwork/2.0
30. *Hagan, M. T., Demuth, H. B., Beale, M. H., Jesús, O.*, Neural Network Design. eBook, 2014.
31. *Razzanelli, M., Pannocchia, G.*, Parsimonious cooperative distributed MPC for tracking piece-wise constant setpoints, IFAC-PapersOnLine **49** (2016) 520. doi: https://doi.org/10.1016/j.ifacol.2016.07.395
32. *Ahmed, D. F., Khalaf, Z. A.*, Artificial neural network control of a multiple effect evaporators via simulation, IOP Conf. Ser. Mater. Sci. Eng. **1094** (2021) 012004. doi: https://doi.org/10.1088/1757-899X/1094/1/012004